MOLECULAR AND CELLULAR BIOLOGY, Sept. 2005, p. 7812–7827 Vol. 25, No. 17
0270-7306/05/$08.00+0 doi:10.1128/MCB.25.17.7812–7827.2005

Complete Loss of *Ndel1* Results in Neuronal Migration Defects and Early Embryonic Lethality

Shinji Sasaki,[1]† Daisuke Mori,[2] Kazuhito Toyo-oka,[2] Amy Chen,[3] Lisa Garrett-Beal,[3] Masami Muramatsu,[1] Shuji Miyagawa,[4] Noriko Hiraiwa,[5] Atsushi Yoshiki,[5] Anthony Wynshaw-Boris,[6] and Shinji Hirotsune[1,2]*

Division of Neuro-Science, Research Center for Genomic Medicine, Saitama Medical School, Yamane 1397-1, Hidaka City, Saitama 350-1241, Japan[1]; Department of Genetic Disease Research, Osaka City University Graduate School of Medicine, Asahi-machi 1-4-3, Abeno, Osaka 545-8586, Japan[2]; Genetic Disease Research Branch, National Human Genome Research Institute, National Institutes of Health, Building 49, Room 4C80, 49 Convent Dr., Bethesda, Maryland 20892[3]; Division of Organ Transplantation, Biomedical Research Center, Osaka University Graduate School of Medicine, 2-2 Yamadaoka, Suita, Osaka 565-0871, Japan[4]; Experimental Animal Division, Department of Biological Systems, BioResource Center, RIKEN Tsukuba Institute, 3-1-1 Koyadai, Tsukuba, Ibaraki 305-0074, Japan[5]; and Departments of Pediatrics and Medicine, UCSD Cancer Center, University of California, San Diego School of Medicine, 9500 Gilman Dr., Mailstop 0627, La Jolla, California 92093-0627[6]

Received 3 March 2004/Returned for modification 28 March 2005/Accepted 8 June 2005

Regulation of cytoplasmic dynein and microtubule dynamics is crucial for both mitotic cell division and neuronal migration. NDEL1 was identified as a protein interacting with LIS1, the protein product of a gene mutated in the lissencephaly. To elucidate NDEL1 function in vivo, we generated null and hypomorphic alleles of *Ndel1* in mice by targeted gene disruption. *Ndel1*$^{-/-}$ mice were embryonic lethal at the peri-implantation stage like null mutants of *Lis1* and cytoplasmic dynein heavy chain. In addition, *Ndel1*$^{-/-}$ blastocysts failed to grow in culture and exhibited a cell proliferation defect in inner cell mass. Although *Ndel1*$^{+/-}$ mice displayed no obvious phenotypes, further reduction of NDEL1 by making null/hypomorph compound heterozygotes (*Ndel1*$^{cko/-}$) resulted in histological defects consistent with mild neuronal migration defects. Double *Lis1*$^{cko/+}$-*Ndel1*$^{+/-}$ mice or *Lis1*$^{+/-}$-*Ndel1*$^{+/-}$ mice displayed more severe neuronal migration defects than *Lis1*$^{cko/+}$-*Ndel1*$^{+/+}$ mice or *Lis1*$^{+/-}$-*Ndel1*$^{+/+}$ mice, respectively. We demonstrated distinct abnormalities in microtubule organization and similar defects in the distribution of β-COP-positive vesicles (to assess dynein function) between *Ndel1* or *Lis1*-null MEFs, as well as similar neuronal migration defects in *Ndel1*- or *Lis1*-null granule cells. Rescue of these defects in mouse embryonic fibroblasts and granule cells by overexpressing LIS1, NDEL1, or NDE1 suggest that NDEL1, LIS1, and NDE1 act in a common pathway to regulate dynein but each has distinct roles in the regulation of microtubule organization and neuronal migration.

The mammalian brain is assembled through a series of far-ranging migrations that result in the segregation of neurons with similar properties into discrete layers (32). Important clues for molecular mechanisms of neuronal migration were provided from the analysis of brain malformations in humans exhibiting neuronal migration defects (13). Lissencephaly is a cerebral cortical malformation characterized by a smooth cerebral surface and a disorganized cortex (3, 4) due to incomplete neuronal migration. In lissencephaly patients, mutation of two genes, *LIS1* or *DCX*, account for the majority of classical lissencephaly (LIS) (31). LIS1 encodes a protein carrying seven WD repeats (33) that was first identified as a noncatalytic subunit of platelet activating factor-acetylhydrolase (Pafah1b1) (15). Consistent with an important role for this protein in neuronal migration, mice with decreased *Lis1* exhibit disorganization of cortical layers, hippocampus, and olfactory bulb in a dose-dependent fashion and are a good model for the human disorder (10, 17). *Lis1*-null mice exhibit peri-implantation lethality and, in *Lis1*-null blastocysts, the inner cell mass degenerated soon after differentiation, suggesting that *Lis1* has an essential role in cell division (17).

LIS1 protein is highly conserved from human to *Aspergillus* (26, 27). The LIS1 homologue in *Aspergillus*, *nudF* (44), was originally identified as a gene mutated in a series of hyphal mutants exhibiting defects in nuclear migration. In addition, *nudF* displayed strong genetic interaction with *nudA* and *nudG*, which encode a cytoplasmic dynein heavy chain (CDHC) and a dynein intermediate chain, respectively (47). CDHC is a microtubule-based minus-end-directed motor protein that plays an important role in mitotic cell division, neuronal migration, and organelle transport (12, 16, 45, 46). Genetic analysis of *Lis1* function in *Drosophila* oogenesis has shown that *Lis1*, similar to cytoplasmic dynein (*Dhc64C*), is essential for germ line cell division and nuclear positioning, supporting the idea that *Lis1* functions with the dynein complex and the microtubule cytoskeleton (20, 21, 40). NudE is an *Aspergillus* gene that genetically interacts with the *nudF*/*Lis1* pathway (6). We and others previously reported that there are

* Corresponding author. Mailing address: Department of Genetic Disease Research, Osaka City University Graduate School of Medicine, Asahi-machi 1-4-3 Abeno, Osaka 545-8586, Japan. Phone: 6-6645-3725. Fax: 6-6645-3727. E-mail: shinjih@med.osaka-cu.ac.jp.

† Present address: Department of Anatomy, Keio University School of Medicine, 35 Shinanomachi, Shinjuku-ku, Tokyo 160-8582, Japan.

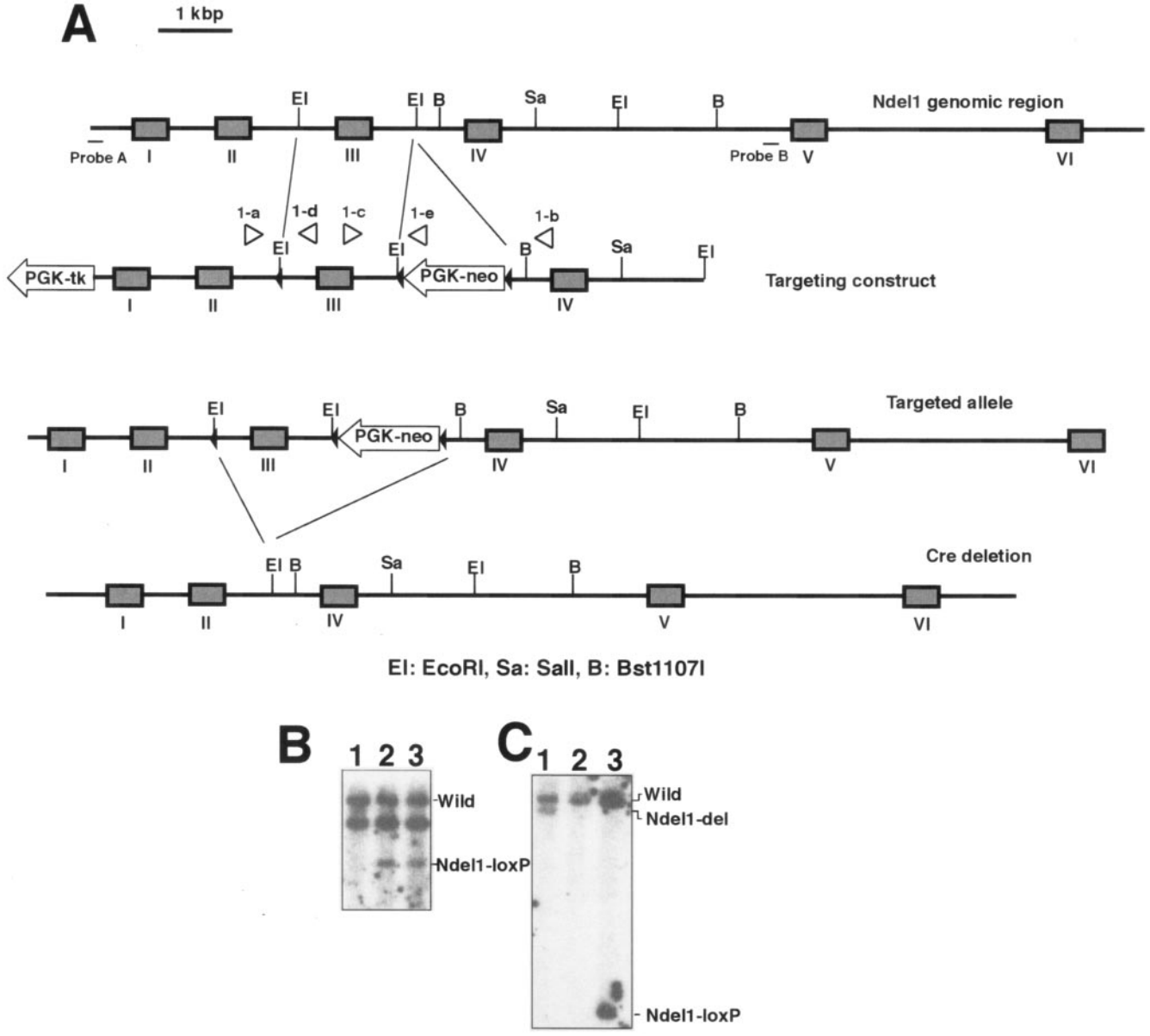

FIG. 1. Generation of a gene-disrupted mouse of *Ndel1* [$Ndel1^{cko(III)}$, $Ndel1^{ko(III)}$]. (A) Summary of targeting strategy for the *Ndel1* locus. A diagrammatic representation of the targeting vector and genomic loci of *Ndel1* gene is shown. Exons are represented by gray boxes. In this gene targeting, *Ndel1* function was expected to be intact ($Ndel1^{cko(III)}$). Exon 3 was removed by CRE-mediated recombination to inactivate *Ndel1* function [$Ndel1^{ko(III)}$]. (B) Southern blot analysis of tail DNA from wild-type (+/+, lane 1) and heterozygous mutant (+/−, lanes 2 and 3) animals. (C) Southern blot analysis of tail DNA from deletion mutant (+/del, lane 1), wild-type (+/+, lane 2), and heterozygous mutant (+/loxP, lane 3) mice. CRE-mediated deletion of exon 3 was evaluated by Southern blotting. Note the difference in band sizes after deletion. We used $Ndel1^{ko(III)}$ as a $Ndel1^{+/-}$ in the all experiment.

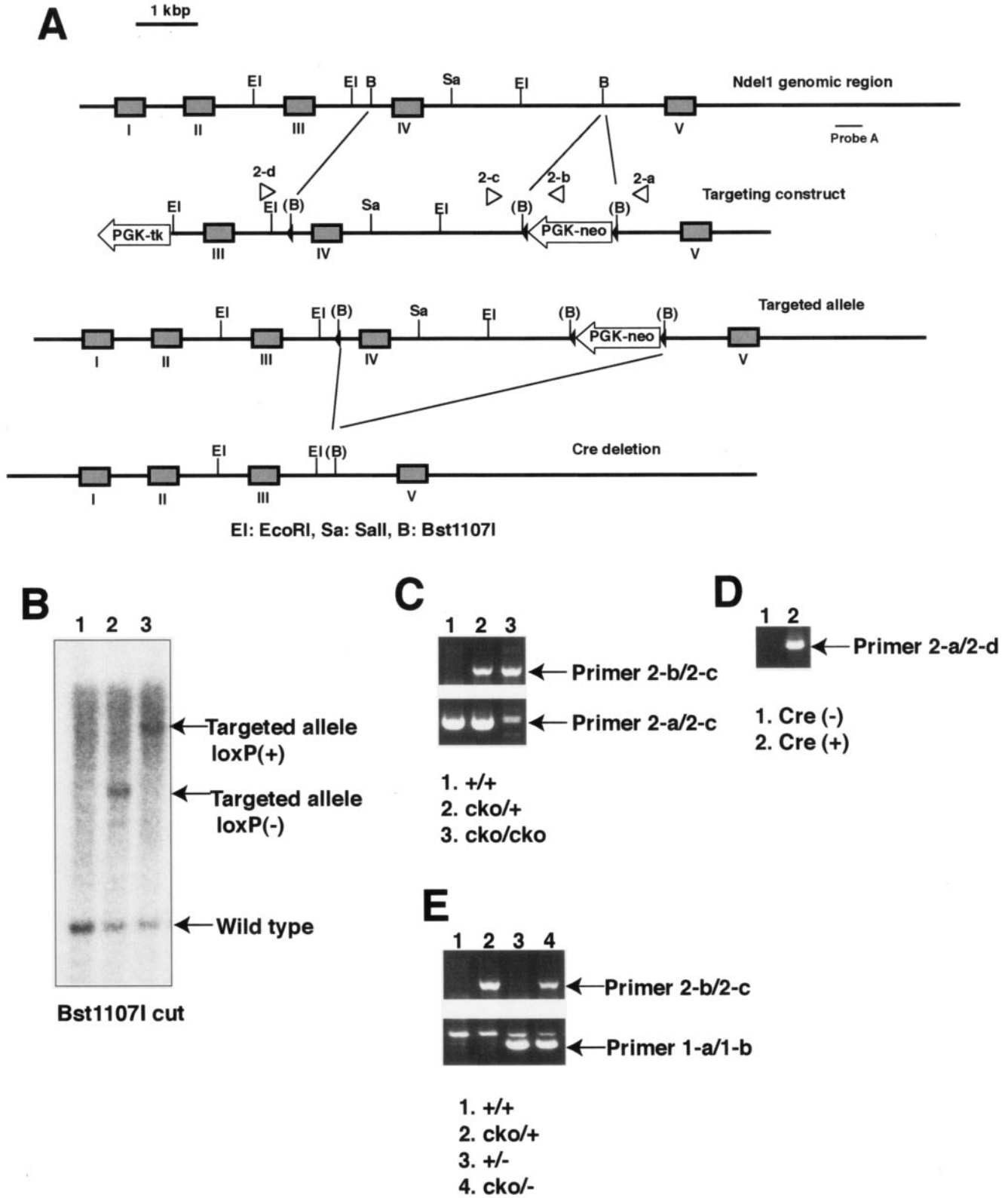

FIG. 2. Generation of another gene disrupted mouse of *Ndel1* [*Ndel1*$^{cko(IV)}$]. (A) Summary of the second targeting strategy for the *Ndel1* locus. A diagrammatic representation of the targeting vector and genomic loci of *Ndel1* gene is shown. *PGK-neo* was inserted into intron IV, which was larger than intron III. Exon IV was removed by CRE-mediated recombination. (B) Southern blot analysis of ES cell DNA. By digestion with Bst1107I, the wild-type allele, the targeted allele that lost the *loxP* site, and the targeted allele that preserved the *loxP* site were discriminated (arrows). (C) Using this conditional KO line, we were able to make conditional homozygotes. Primers are shown on the right side (arrows). (D) CRE expression efficiently removed the DNA fragment that was demarcated by *loxP* sequence. (E) We mated new conditional KO mice and KO mice to make compound heterozygotes. Primers are shown on the right side. Compound heterozygotes were completely viable and fertile. We used *Ndel1*$^{cko(IV)}$ as *Ndel1*$^{cko/+}$ in all experiments.

TABLE 1. Embryos and mice used in this study

Embryo (days p.c.) or mouse[a]	No.[b]	Genotype[c]			No. resorbed
		+/+	+/−	−/−	
Embryos					
7.5	10	4	6	0	0
8.5	7	2	5	0	0
9.5	9	4	5	0	0
10.5	10	4	6	0	0
11.5	12	3	9	0	0
12.5	17	5	12	0	0
13.5	15	4	11	0	0
Total	80	26	54	0	0
Mice					
Newborn	57	19	38	0	
Weaning	167	51	116	0	
Total	224	70	154	0	

[a] Newborn mice were genotyped within 12 h of birth. Weaning mice were typically 4 weeks of age. p.c., postcoitus.
[b] The number of embryos includes the number resorbed.
[c] Genotypes for embryos were determined by PCR analysis of tissue lysate of blastocyte outgrowth for E3.5 and of yolk sac for E7.5 to E13.5. Genotypes for newborn and weaning mice were determined by PCR analysis of tail DNA.

two mammalian homologues of *Aspergillus NudE*, NDE1 (8) and NDEL1 (29, 35, 36); the latter, a homologue of *NudE* from *Aspergillus nidulans*, is a LIS1 binding protein that participates with LIS1 in the regulation of CDHC function via phosphorylation by CDK5/p35 (8, 29, 35, 36), a complex known to be essential for neuronal migration (1, 7, 11, 13, 18, 30). We have also shown that phosphorylation of NDEL1 is protected by the serine-threonine binding protein 14-3-3ε and that 14-3-3ε is required for normal neuronal migration (42), providing further support that the phosphorylation of NDEL1 is required for proper neuronal migration. NDE1 has a similar function in cells but is expressed later in development than NDEL1. Recently, *Nde1*-null mice have been produced (9). These mice are viable and display microcephaly. They display defects in neurogenesis that result from reduced progenitor cell division and progenitor cell fate, as well as modest defects in neuronal migration. To date, targeted mutants of *Ndel1* have not been generated, and the in vitro phenotype of null mutants of *Ndel1* is unknown.

To understand the role of NDEL1 in vivo and to determine whether it plays a role in corticogenesis and cell division, we generated *Ndel1*-disrupted mice. We found that, similar to *Lis1*, *Ndel1* mutant mice display a dosage-dependent neuronal migration phenotype, and complete loss of *Ndel1* resulted in perinatal lethality. Examination of in vivo and in vitro phenotypes suggests that NDEL1, LIS1, and NDE1 act in a common pathway to regulate dynein, but each has distinct roles in the regulation of microtubule organization and neuronal migration.

MATERIALS AND METHODS

Generation and analysis of *Ndel1* KO mice. To understand the function of *Ndel1* in vivo, we generated a first conditional knockout (KO) mouse to inactivate *Ndel1* by Cre-mediated recombination. We assembled a targeting construct in which a *PGK-neo* gene flanked by a *loxP* site and an additional *loxP* site were inserted into intron III and intron II, respectively. The linearized targeting construct was introduced into TC1 embryonic stem (ES) cells (2) from a 129S6 background by electroporation. The targeted ES clones were screened by Southern blot and injected into blastocysts to create chimeric mice. Highly agouti chimeric males were mated to wild-type females to give rise to heterozygotes for the conditional allele [$Ndel1^{cko(III)/+}$], which was identified by Southern blot analysis and PCR. These heterozygous mice were mated with *EIIa-Cre* germ line deleter transgenic mice (19). Offspring from the matings between an $Ndel1^{cko(III)/+}$ line and an *EIIa-Cre* transgenic line were genotyped by Southern blot analysis and PCR. Southern blot analysis and PCR examination indicated efficient deletion of the fragment carrying exon III by CRE mediated recombination in vivo. $Ndel1^{cko(III)/cko(III)}$ mice exhibited embryonic lethality similar with $Ndel1^{ko(III)/ko(III)}$ mice, suggesting that the presence of the neo gene severely affects expression of *Ndel1*. It was not possible to remove neo gene by itself. For the second conditional KO strategy, we inserted a PGK-neo gene flanked by a *loxP* site and an additional *loxP* site into intron IV and intron III, respectively. Highly agouti chimeric males were mated to wild-type females to give rise to heterozygotes for the second conditional allele [$Ndel1^{cko(IV)/+}$]. In contrast to the first line of conditional KO, homozygotes of the second conditional KO [$Ndel1^{cko(IV)/cko(IV)}$] line was completely viable and fertile. CRE-mediated deletion of the second conditional KO mouse line was also confirmed by PCR with primers located flanking the site of the deleted region. We used $Ndel1^{ko(III)/+}$ as $Ndel1^{+/-}$, whereas $Ndel1^{cko(IV)/+}$ was used as $Ndel1^{cko/+}$ in this experiment. Expression of NDEL1 was examined by Western blotting with the C-6 NDEL1 specific antibody (36) and Northern blotting with a full-length *Ndel1* cDNA fragment. All experiments with mouse models were performed based on the animal experiment guidelines of our universities.

BrdU birth dating study. For bromodeoxyuridine (BrdU) experiments, pregnant dams (embryonic day 15.5 [E15.5]) were injected with BrdU (50 μg/g, intraperitoneally). Subsequently, the distribution of BrdU-positive cells was determined at P0. The incorporation of BrdU in cells was detected with a mouse anti-BrdU monoclonal primary antibody (Roche), followed by an alkaline phosphatase-conjugated secondary antibody (Boehringer Mannheim). We analyzed three independent mice for each genotype.

Histological examination and immunohistochemistry. After perfusion with Bouin's or 4% paraformaldehyde fixative, tissues from wild-type and various mutant mice were subsequently embedded in paraffin and sectioned at 5-μm thickness. After deparaffination, endogenous peroxidase activity was blocked by incubating the sections in 1.5% peroxide in methanol for 20 min. The sections were then boiled in 0.01 mol of citrate buffer (pH 6.0)/liter for 20 min and cooled slowly. Before staining, the sections were blocked with rodent block (LabVision) for 60 min. The sections were washed in phosphate-buffered saline and incubated with each antibody. Primary cultures of cerebellar granule cells were generated from 5-day-old C57BL/6 pups as described previously (36). Cells were plated at a density of 2.5×10^5 cells/cm^2 and maintained in basal Eagle medium containing 10% fetal calf serum, 25 mM KCl, 2 mM glutamine, and 50 mg of gentamicin/ml. After 18 to 20 h, cytosine arabinoside (10 mM) was added to the culture media to halt non-neuronal cell proliferation. Blastocysts were collected by flushing the oviducts of female mice at 3.5 days postcoitum and cultured individually for 3 days on gelatinized coverslips in ES cell medium. Cultured blastocysts were fixed in 2% paraformaldehyde–phosphate-buffered saline for 10 min at room temperature. Some samples were fixed in 2% paraformaldehyde and 0.2% glutaraldehyde for 10 min at room temperature and blocked in 1 mg of $NaBH_4$/ml for 30 min at 4°C. After primary culture from each tissue, cells were fixed in cold methanol (−20°C) and postfixed by 3% formaldehyde. Incubation with 0.15% Triton X-100 was used for cell permeabilization after fixation. Immunohistochemistry was performed based on the standard procedure. Apoptotic cells were detected by TUNEL (terminal deoxynucleotidyltransferase-mediated dUTP-biotin nick end labeling) assay (Chemicon). Incorporated biotin was detected with an ABC kit and visualized with diaminobenzidene.

Primary cell culture, transfection, and immunofluorescence. Establishment of mouse embryonic fibroblasts (MEFs) was performed as previously described (17, 36). A red fluorescent protein (RFP)-tagged *Cre* expression vector was introduced into these primary culture cells by using Lipofectamine 2000 reagents (Invitrogen). After CRE-mediated inactivation of *Lis1* or *Ndel1* gene, these cells were subjected to immunohistochemistry by using anti-β-tubulin antibody (Clone TUB 2.1; Sigma) or anti-β-COP antibody (Sigma). For rescue experiments, green fluorescent protein (GFP)-conjugated to LIS1, NDEL1, or NDE1 was simultaneously transfected with the CRE expression vector.

Reaggregate neuronal migration assay. Cerebellar granule neurons were dissociated from postnatal 5-day-old mice (17, 41) and transfected with various vectors by using LipoTrust SR transfection reagents (Hokkaido System Science Co., Ltd.) according to the manufacturer's instructions with a small modification. Briefly, 2×10^6 cells were transfected with 3 μg of DNA vector in 4 μl of LipoTrust SR reagents in 100 μl of Dulbecco modified Eagle medium media without fetal bovine serum for 20 h, resulting in 30 to 40% transfection efficiency. Reaggregates were transferred to poly-L-lysine (Sigma-Aldrich)- and laminin

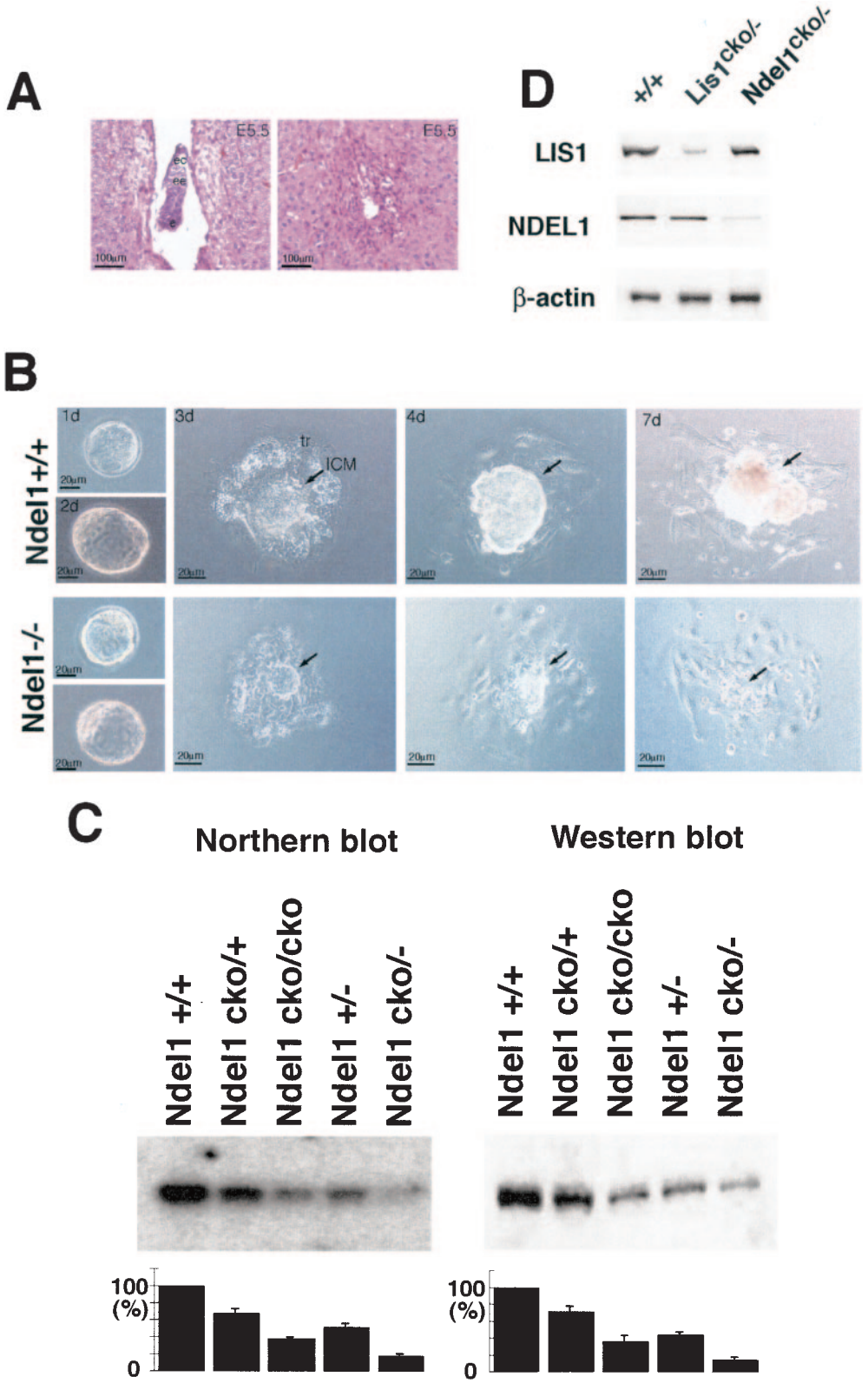

FIG. 3. Embryonic lethality of *Ndel1*-null mutants. (A) Homozygous mutants of *Ndel1* were not observed, suggesting that null mutants are embryonic lethal. Normal (left) and degenerated deciduas (right) resulting from the *Ndel1*$^{+/-}$ cross were sectioned at E5.5 and stained with hematoxylin and eosin. ec, ectoplacental cone; ee, extra-embryonic ectoderm; e, epiblast. (B) Wild-type (upper) and homozygous (lower) blastocysts were isolated from a heterozygous cross and cultured. Both blastocysts hatched and differentiated into trophoblast (tr) and inner cell mass (ICM). The inner cell mass of homozygotes exhibited poor growth and degenerated. (C) Quantitation of the amount of Ndel1 expression in the various genotypes. Northern blot (left side) and Western blot (right side) are shown. Expression was calculated by densitometry compared to the wild type. We repeated three independent experiments, and the results were highly reproducible. (D) Expression of LIS1 or NDEL1 in *Ndel1* KO mice or *Lis1* KO mice was examined. Total protein was extracted from a brain of E15.5 embryo and subjected to Western blotting. There was no obvious difference in LIS1 or NDEL1 expression in *Ndel1* or *Lis1* KO mice, respectively.

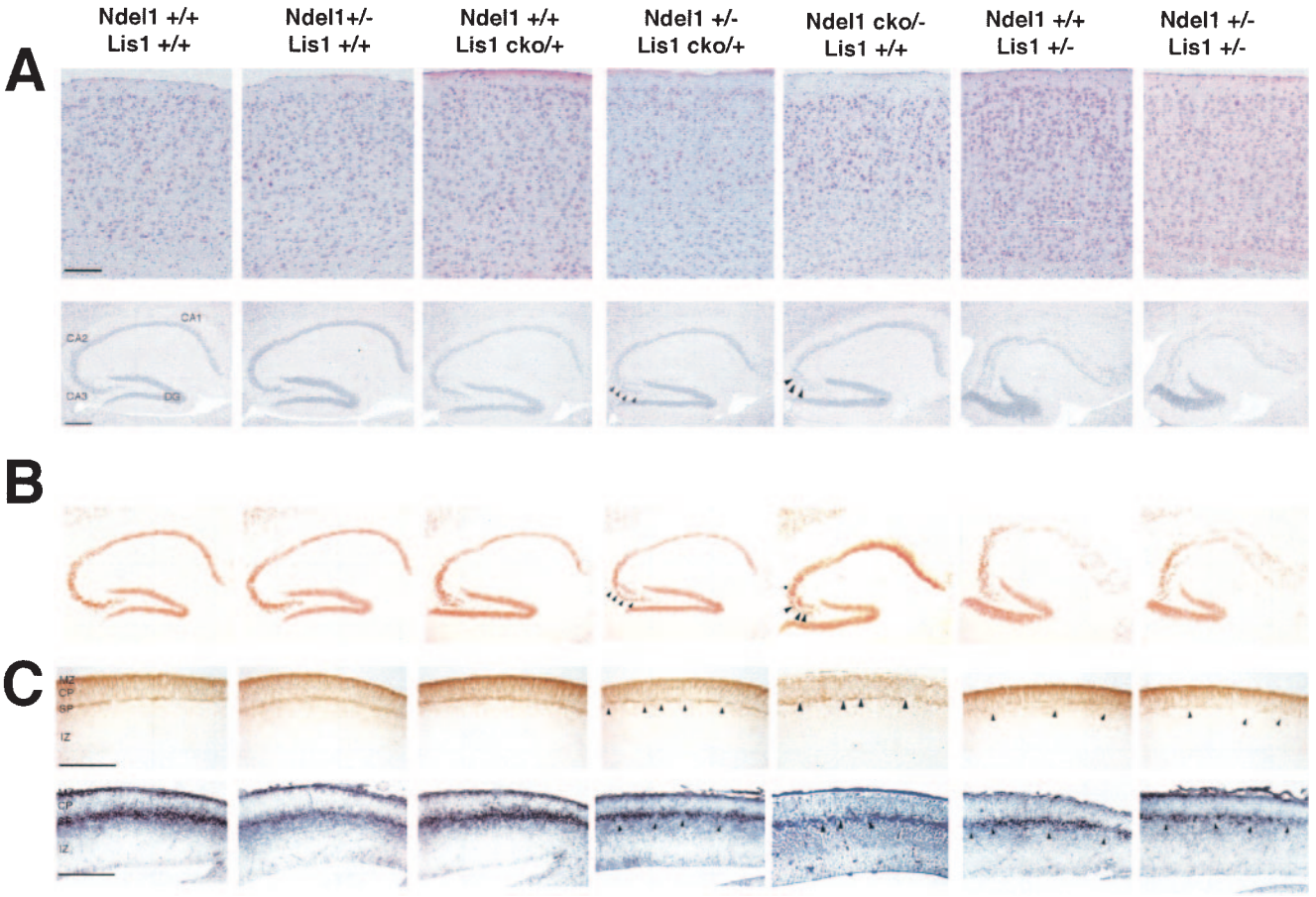

FIG. 4. Synergistic effects of *Lis1* and *Ndel1* mutations on brain morphogenesis. Genotypes are shown at the top of the panels. (A) Midsagittal sections of cerebral cortex (upper) and hippocampus (lower). $Lis1^{cko/+}$ or $Ndel1^{+/-}$ samples were grossly normal. In contrast, mild cell dispersion of CA3 region was observed in $Ndel1^{cko/-}$ compound heterozygotes or $Lis1^{cko/+}$ and $Ndel1^{+/-}$ double heterozygotes (arrowheads). (B) Loss of cell compaction (arrowheads) in CA3 region was clearly observed by NeuN staining. (C) Abnormal corticogenesis was characterized by fragmentation of the subplate layer (arrowheads) which was visualized by MAP2 staining (upper panels) and chondroitin sulfate proteoglycan staining (lower panels) at E15.5. MZ, marginal zone; CP, cortical plate; SP, subplate; IZ, intermediate zone.

(Sigma-Aldrich)-treated slides. After 15 h, the distance between cell bodies and the edge of reaggregates was measured. The details of the experimental procedure have been described (17, 41). An RFP-tagged *Cre* expression vector with or without GFP-tagged LIS1, NDEL1, or NDE1 vector were transfected as described above.

RESULTS

Targeted gene disruption of *Ndel1*. To explore the in vivo role of NDEL1 and genetic interaction between *Ndel1* and *Lis1* during mitotic cell division and neuronal development, we generated two independent *Ndel1* conditional KO lines (Fig. 1 and Fig. 2; see also Materials and Methods). We could not delete the *PGK-neo* gene used for selection in ES cells in the exon III floxed allele, and the undeleted allele with the *neo* insertion had a homozygous lethal phenotype identical to that of the null allele produced after deletion of the *PGK-neo* gene and exon III (see Materials and Methods). Therefore, we produced a conditional allele that floxed exon IV. We used mice in which exon III of *Ndel1* was deleted as $Ndel1^{+/-}$, whereas we used mice in which exon IV of *Ndel1* was conditionally deleted as $Ndel1^{cko/+}$.

Mice heterozygous for the *Ndel1* gene ($Ndel1^{+/-}$) were outwardly normal, fertile born in appropriate Mendelian ratios. $Ndel1^{+/-}$ mice were bred to produce homozygous mutants ($Ndel1^{-/-}$). An analysis of F_2s from the mating of $Ndel1^{+/-}$ mice showed that the genotype ratios of +/+ to +/− to −/− animals were 70:154:0, suggesting that the complete loss of *Ndel1* resulted in embryonic lethality (Table 1). Therefore, we examined embryos from heterozygous crosses at several developmental stages. Cumulative genotyping between E7.5 and E13.5 demonstrated that the ratios of +/+ to +/− to −/− mice were 26:54:0 (Table 1). We dissected embryos at between E5.5 and E13.5 and found degenerated embryos and empty deciduas only at the earliest postimplantation stages (Fig. 3A). We found 35 normal embryos (80%) and 10 empty decidua (20%) at E5.5 among 45 animals, and there were 5 +/+ (21%), 15 +/− (66%), and 3 −/− (13%) blastocyst cultures at E3.5 among 23 animals. These findings suggested that $Ndel1^{-/-}$ mice are lethal at very early stages of embryogenesis. This is in contrast to *Nde1*-null mice, which are viable and display microcephaly from defects in neurogenesis (9).

To define the role of NDEL1 in the early embryo, we examined the behavior of blastocyst explants isolated from

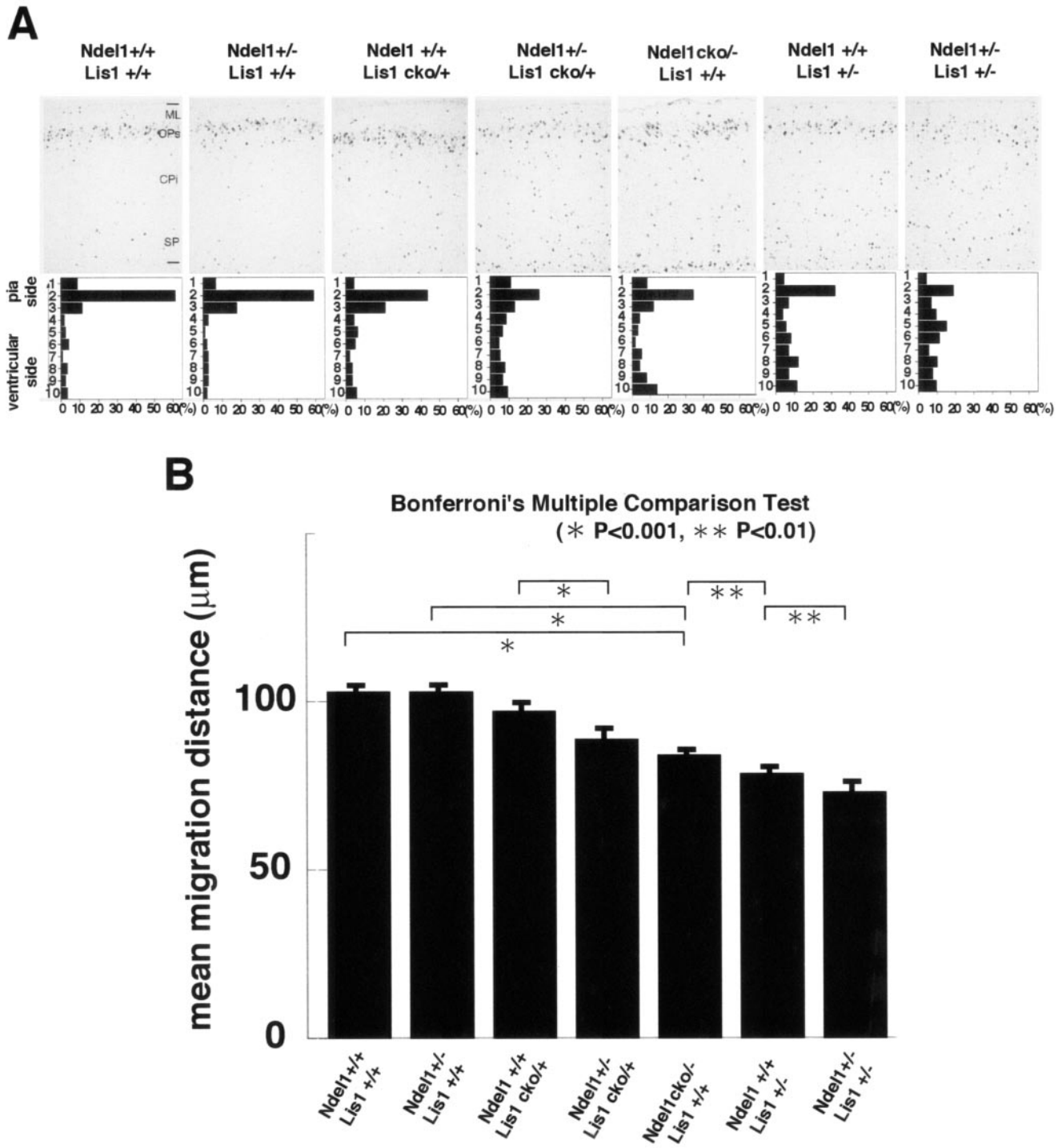

FIG. 5. Examination of migration defects of *Lis1* and *Ndel1* mutants. (A) BrdU birth dating analysis reveals neuronal migration defects in the cross of $Ndel1^{+/-}$ and $Ndel1^{cko/+}$, in the cross of $Lis1^{cko/+}$ and $Ndel1^{+/-}$, or in the cross of $Lis1^{+/-}$ and $Ndel1^{+/-}$. Genotypes are described at the top of the panels. Mice were injected with BrdU at E15.5 and sacrificed at P0. Quantitative analysis was performed by measuring the distribution of BrdU-labeled cells in each bin which equally divided the cortex from the molecular layer (ML) to the subplate (SP). The staining patterns are representative of three different experiments. Note the shift downward toward the ventricular side as *Lis1* or *Ndel1* dosage was reduced. CPs, cortical plate surface; CPi, cortical plate inner. (B) Summary of mean migration distance of each genotype.

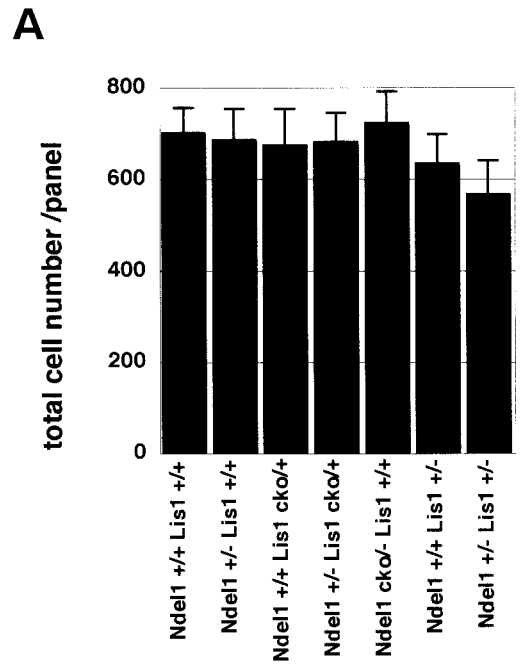

FIG. 6. Specific defect of corticogenesis and apoptotic cell death by *Lis1* or *Ndel1* disruption. (A) Quantitation of cell number of the cortex in various combination of *Lis1* KO and/or *Ndel1* KO mice. After hematoxylin and eosin staining of the sagittal sections of the cortexes of 8W adult mice, samples were subjected to cell counting. The cell counts of three corresponding sections in each genotype were determined. The histogram indicates the cell number. Mild reduction of cell number was observed in $Lis1^{+/-}/Ndel1^{+/+}$ and $Lis1^{+/-}/Ndel1^{+/-}$ mutants. (B) Cortical phenotypes of *Lis1* and/or *Ndel1* mutants (adult, 8W) were examined by layer specific makers, calbindin (layer 2 and 3) and c-Neu (layer 5). We measured five independent sides from each genotype. Total number of calbindin-positive cells is shown at the bottom of each panel. Calbindin-positive cells were more dispersed in $Ndel1^{+/-}/Lis1^{cko/+}$, $Ndel1^{cko/-}/Lis1^{+/+}$, $Ndel1^{+/+}/Lis1^{+/-}$, and $Ndel1^{+/-}/Lis1^{+/-}$ mice, whereas c-Neu-positive cells were more broadly distributed in $Ndel1^{cko/-}/Lis1^{+/+}$, $Ndel1^{+/+}/Lis1^{+/-}$, and $Ndel1^{+/-}/Lis1^{+/-}$ mice. Although the distribution became more broad and overlapped, inversion of layering was not observed. Genotypes are noted at the top of the panel. (C) Histogram plots of the relative frequency of calbindin-positive cells and c-Neu-positive cells to the total cell number in each genotype. Notably, later-migrating neurons (calbindin-positive cells) were more sensitive to LIS1 and NDEL1 dosage. (D) Apoptotic cell death was examined by TUNEL stainong at E11.5 and E15.5. We measured five independent sides from each genotype. The total number of calbindin-positive cells is shown at the bottom of each panel. (E) Histogram plot of the relative frequency of TUNEL-positive cell to the total number of cells in each genotype. There was no obvious increase of cell death in early generated neurons. In contrast, significant enhancement of cell death was observed in neurons generated later, a finding consistent with loss of calbindin-positive cells, and cell death was highly correlated with the reduction of LIS1 dosage.

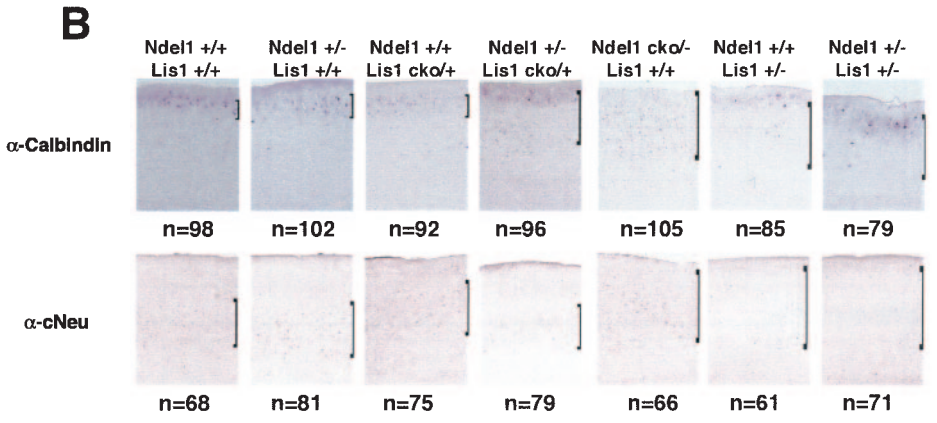

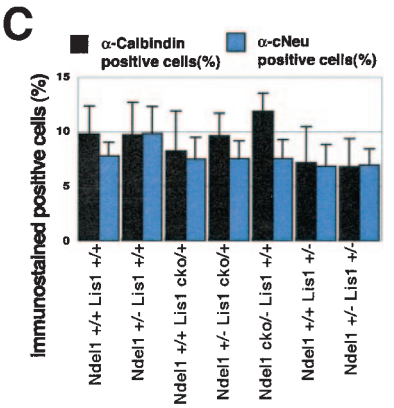

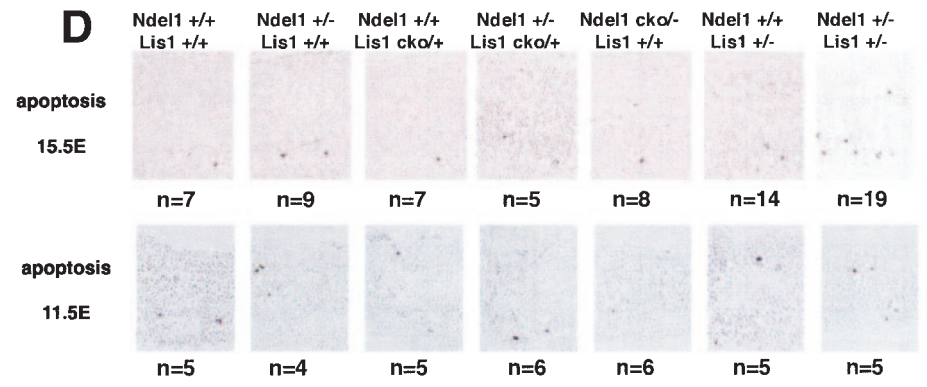

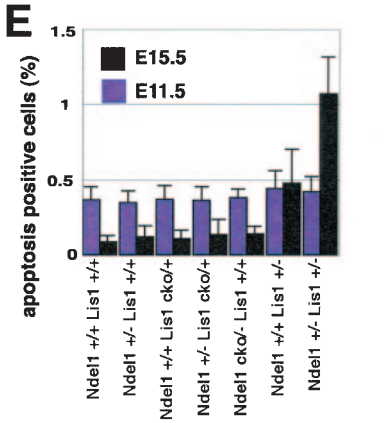

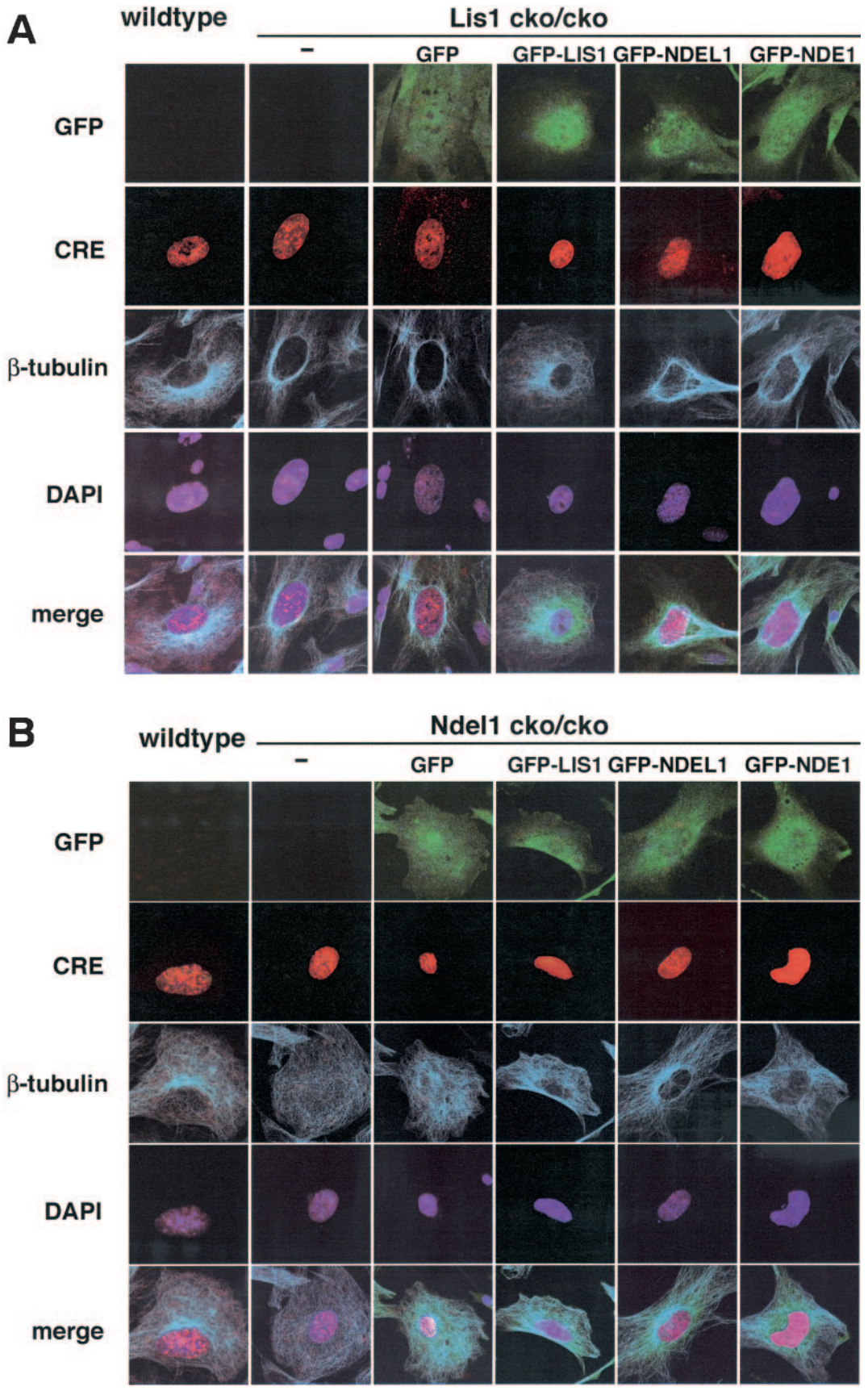
A
wildtype
Lis1 cko/cko
–
GFP
GFP-LIS1
GFP-NDEL1
GFP-NDE1
GFP
CRE
β-tubulin
DAPI
merge
B
wildtype
Ndel1 cko/cko
–
GFP
GFP-LIS1
GFP-NDEL1
GFP-NDE1
GFP
CRE
β-tubulin
DAPI
merge

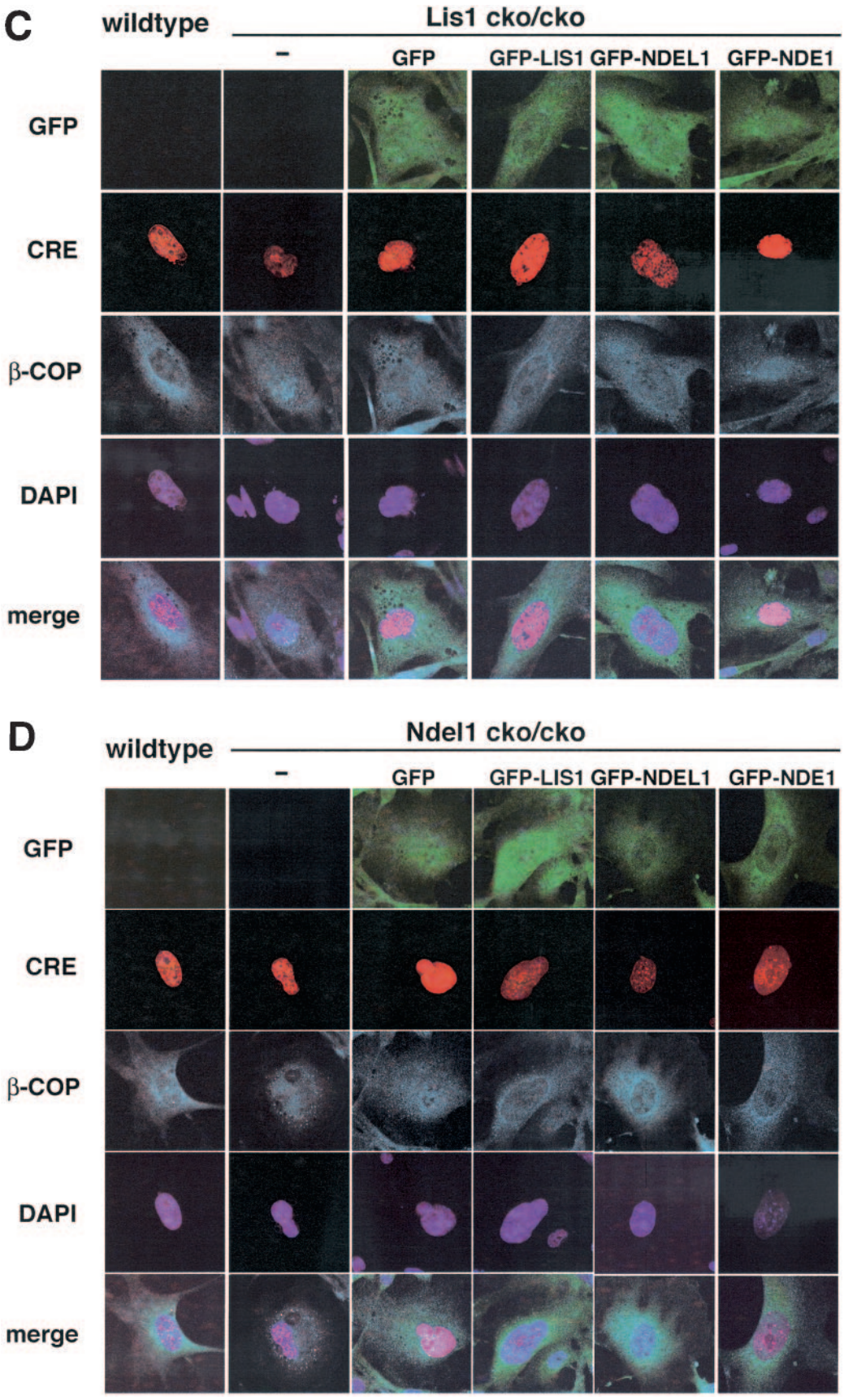
C
wildtype
Lis1 cko/cko
–
GFP
GFP-LIS1
GFP-NDEL1
GFP-NDE1
GFP
CRE
β-COP
DAPI
merge
D
wildtype
Ndel1 cko/cko
–
GFP
GFP-LIS1
GFP-NDEL1
GFP-NDE1
GFP
CRE
β-COP
DAPI
merge

Ndel1$^{+/-}$ crosses in culture. Genotypes of explants were performed by PCR at the end of the experiment. Wild-type, heterozygous (data not shown), and homozygous blastocysts attached to the substratum. Trophoblast cells from wild-type blastocyst explants flattened and expanded, while the inner cell mass grew on the top of the trophoblast cells (Fig. 3B). In contrast, the inner cell mass cells of *Ndel1*$^{-/-}$ blastocyst explants grew poorly after 3 days and degenerated soon thereafter. These phenotypes were previously observed in *Lis1* or *CDHC* KO mice (14, 17).

We quantitated *Ndel1* mRNA and protein expression by Northern (Fig. 3C, left) blotting and Western blotting (Fig. 3C, right), respectively. Insertion of the *neo* gene into intron IV partially suppressed *Ndel1* expression (30%), demonstrating that the conditional allele which carries the *neo* gene acts as a hypomorphic mutant. To test whether either *Lis1* or *Ndel1* inactivation results in altered expression of NDEL1 or LIS protein, respectively, we examined LIS1 in *Ndel1*-disrupted mice or NDEL1 in *Lis1*-disrupted mice (Fig. 3D). There was no obvious effect on expression of NDEL1 or LIS1 protein by *Lis1* or *Ndel1* disruption, respectively.

Neuronal migration defect in *Ndel1* disrupted mice and genetic interaction with *Lis1*. In the adult brain (8W), *Ndel1*$^{+/-}$ mice displayed no obvious migration defects in either the neocortex or hippocampus (Fig. 4A). We further reduced the level of NDEL1 expression to ca. 20% of wild-type by making compound heterozygotes (*Ndel1*$^{cko/-}$). *Ndel1*$^{cko/-}$ mice exhibited mild partial splitting and diffuse pyramidal cells in the CA3 and CA2 region of the hippocampus (Fig. 4A). To examine genetic interaction between *Ndel1* and *Lis1*, we mated *Ndel1*$^{+/-}$ mice to *Lis1*$^{cko/+}$ mice or *Lis1*$^{+/-}$ mice. Although *Lis1*$^{+/-}$ mice displayed their typical migration defect (17), *Lis1*$^{cko/+}$ mice showed overall fairly normal brain morphology. In contrast to single heterozygotes, the pyramidal cells in the CA3 region of the hippocampus were partially split in *Ndel1*$^{+/-}$/*Lis1*$^{cko/+}$ double heterozygotes (Fig. 4A). *Lis1*$^{+/-}$ mice displayed severe migration defects in the hippocampus recognized by the splitting of pyramidal cells. These migration defects appeared to be slightly more severe in *Ndel1*$^{+/-}$/*Lis1*$^{+/-}$ double heterozygotes. These results suggested that *Ndel1* and *Lis1* genetically interacted during neuronal migration. The abnormal layering in the hippocampus was also clearly visualized by NeuN staining, a marker for terminal differentiation of neurons (Fig. 4B) (28). We assessed defects in cortical architecture and fragmentation of the subplate by immunohistochemical analysis with MAP2, which specifically identifies dendritic extensions of postmitotic neurons. In wild-type and *Lis1*$^{cko/+}$ embryos, MAP2-positive neuronal processes were arranged radially to form a tight, palisade-like pattern at the cortical plate (Fig. 4C, upper panels). MAP2 also stains the horizontal processes of subplate neurons (23) but not those in the intermediate zones (34). In contrast, radial and palisade staining of the cortical plate became irregular, and horizontal staining of the subplate was fragmented in *Ndel1*$^{cko/-}$, *Ndel1*$^{+/-}$/*Lis1*$^{cko/+}$, and *Ndel1*$^{+/-}$/*Lis1*$^{+/-}$ double heterozygotes compared to *Ndel1*$^{+/-}$ or *Lis1*$^{cko/+}$ single heterozygotes. Chondroitin sulfate proteoglycan is distributed in the marginal zone and the subplate (37). This marker also revealed fragmentation and abnormal organization of the subplate from *Ndel1*$^{cko/-}$ mice (Fig. 4C, lower panels). Consistent with the biochemical interaction of LIS1 and NDEL1 (36), these developmental studies further suggest that *Lis1* and *Ndel1* genetically interact and synergistically regulate neuronal migration.

BrdU birth dating analysis of *Ndel1*-disrupted mice and genetic interaction with *Lis1*. To confirm that the morphological defects observed in the several genetic combinations were due to abnormal neuronal migration, we performed quantitative BrdU birth dating analysis on each genetic combination. As the dose of NDEL1 was reduced, the distribution of labeled cells was shifted downward toward the ventricular zone in the cortex, and BrdU labeling was more diffusely localized (Fig. 5A, *Ndel1*$^{cko/-}$/*Lis1*$^{+/+}$). The migration defects associated with the reduction of NDEL1 became more severe in the presence of reduced levels of LIS1 (Fig. 5A, *Ndel1*$^{+/-}$/*Lis1*$^{cko/+}$) compared to *Ndel1*$^{+/-}$ or *Lis1*$^{cko/+}$ mutants. Although *Lis1*$^{+/-}$ mutants displayed migration defects, additional heterozygous loss of NDEL1 significantly reduced the cell population that reached layer II (Fig. 5A, *Ndel1*$^{+/-}$/*Lis1*$^{+/-}$). Although heterozygous loss of NDEL1 was not sufficient for the creation of a clear migration defect as in the *Lis1*$^{+/-}$ mutants, combinatorial loss of *Ndel1* and *Lis1* clearly led to a migration defect (Fig. 5B), suggesting that LIS1 and NDEL1 cooperatively function during neuronal migration in the cortex, as well as in the hippocampus.

Apoptotic cell death in *Ndel1*-disrupted mice and *Lis1* mutants. We observed mild reduction of the density of cells in the neocortex of the *Ndel1*$^{+/+}$/*Lis1*$^{+/-}$ mice and the *Ndel1*$^{+/-}$/*Lis1*$^{+/-}$ mice (Fig. 6A). To determine potential defects of corticogenesis due to reduction of LIS1 and/or NDEL1, we analyzed C-Neu immunoreactivity to label the large pyramidal neurons of layer 5 (43) and calbindin immunoreactivity to label the interneurons of layers 2 and 3 (24) in the adult cortex (8W) of these different crosses (Fig. 6B). C-Neu-positive cells that migrate at an early stage exhibited broader distribution in

FIG. 7. Disruption of microtubule organization and distribution of β-COP-positive vesicles in *Lis1*- or *Ndel1*-null MEFs. Aberrant microtubule organization and abnormal distribution of β-COP-positive vesicles in *Lis1* or *Ndel1*-null MEFs generated by CRE-mediated recombination. Cotransfected plasmids for rescue were shown on the top. (A and B) The loss of LIS1 causes a redistribution and an enrichment of microtubules near the nucleus (A), whereas loss of NDEL1 results in amorphous microtubules (B). Perinuclear accumulation of microtubules in *Lis1*-null MEFs was only rescued by GFP-LIS1 expression (see panel A). GFP-NDEL1 expression also rescued the amorphous microtubule organization in *Ndel1*-null MEFs, but GFP-LIS1 and GFP-NDE1 were less effective (see panel B). To address dynein regulation by LIS1 and NDEL1, we examined the distribution of β-COP-positive vesicles, which display juxtanuclear localization in a dynein-dependent fashion. (C and D) The predominant juxtanuclear staining pattern was disrupted in *Lis1*-null MEFs (C) and in *Ndel1*-null MEFs (D), resulting in a homogeneous distribution accompanied by punctuate accumulation. Loss of this Golgi pattern by *Lis1* inactivation was only rescued by exogenous expression of GFP-LIS1 (see panel C). In contrast, loss of the Golgi pattern by *Ndel1* inactivation was efficiently rescued by exogenous expression of GFP-LIS1, GFP-NDEL1, and GFP-NDE1 (see panel D).

Ndel1$^{cko/-}$/*Lis1*$^{+/+}$, *Ndel1*$^{+/+}$/*Lis1*$^{+/-}$, and *Ndel1*$^{+/-}$/*Lis1*$^{+/-}$ genotypes, whereas calbindin-positive cells which migrate at a later stage exhibited broader distribution in *Ndel1*$^{+/-}$/*Lis1*$^{cko/+}$, *Ndel1*$^{cko/-}$/*Lis1*$^{+/+}$, *Ndel1*$^{+/+}$/*Lis1*$^{+/-}$, and *Ndel1*$^{+/-}$/*Lis1*$^{+/-}$ genotypes, suggesting that later migrating neurons are more sensitive to reduction of LIS1 and/or NDEL1. Quantitation of densities indicated mild reduction of calbindin-positive cells in the cortexes of the *Ndel1*$^{+/+}$/*Lis1*$^{+/-}$ mice and the *Ndel1*$^{+/-}$/*Lis1*$^{+/-}$ mice, whereas C-Neu positive cells did not display obvious genotype-dependent differences (Fig. 6C). These results prompted us to investigate apoptotic cell death during corticogenesis in various crosses by TUNEL (terminal deoxynucleotidyltransferase-mediated dUTP-biotin nick end labeling) staining (Fig. 6D). At E11.5 when early migrating neurons are generated, significant differences of apoptotic cell death were not observed. In contrast, at E15.5 when later migrating neurons are generated, significant acceleration of apoptotic cell death in the ventricular zone were observed. In particular, cell death was correlated with the reduction of LIS1 amount, a finding in good agreement with the reduction of calbindin-positive cells in the cortexes of the *Ndel1*$^{+/+}$ *Lis1*$^{+/-}$ mice and *Ndel1*$^{+/-}$ *Lis1*$^{+/-}$ mice (Fig. 6E).

Abnormal organization of microtubules and distribution of β-COP-positive vesicles in *Lis1*- or *Ndel1*-null MEFs. We next addressed LIS1 and NDEL1 functions on microtubule organization and dynein regulation. In wild-type MEFs, microtubule arrays were displayed throughout the cell from a clear focus that likely represented the centrosome (Fig, 7A). Loss of either *Lis1* or *Ndel1* caused profound changes in the organization of microtubules of MEFs. Microtubules exhibited a perinuclear concentration in *Lis1*-disrupted MEFs (39) (Fig. 7A). This aberrant distribution of microtubules in *Lis1*-null MEFs was only rescued by exogenous GFP-LIS1 expression (Fig. 7A) but not by GFP-NDEL1 or GFP-NDE1. In contrast, microtubules in *Ndel1*-disrupted MEFs displayed an amorphous and fragile pattern (Fig. 7B). Similarly, the microtubule organization defect in *Ndel1*-null MEFs was efficiently rescued by GFP-NDEL1 but not by either LIS1 or NDE1, which only slightly rescued the disorganization of microtubules (Fig. 7B). Based on the different phenotypes in *Lis1*- and *Ndel1*-null MEFs, these data suggest that NDEL1 plays a distinct role in the regulation of microtubule organization.

We also examined the distribution of β-COP-positive vesicles. β-COP proteins are part of a coatomer complex that recruits some specific areas of the endomembrane system to the Golgi complex in a cytoplasmic dynein-dependent fashion (5). Immunofluorescence demonstrated that β-COP-positive vesicles displayed a predominantly juxtanuclear staining pattern in wild-type MEFs (Fig. 7C). Upon inactivation of *Lis1* or *Ndel1* by CRE recombinase, this clustering in the juxtanuclear region was disrupted, and β-COP was redistributed homogeneously within the cell accompanied by a punctuate accumulation (Fig. 7C and D). Aberrant distribution of β-COP positive vesicles in *Lis1*-null MEFs was only rescued by exogenous introduction of GFP-LIS1 (Fig. 7C). In contrast, disrupted organization of of β-COP-positive vesicles in *Ndel1*-null MEFs was efficiently rescued by GFP-NDE1, as well as GFP-NDEL1, and it was partially rescued by GFP-LIS1 (Fig. 7D). These data suggest that LIS1, NDEL1, and NDE1 share some overlapping and some distinct functions in the regulation of cytoplasmic dynein function.

Neuronal migration defects in *Lis1* and *Ndel1* mutant granule cells. To define the mechanistic roles of NDEL1 and LIS1 in mammalian neuronal migration, we used mouse cerebellar granule neurons in an in vitro migration assay with wild-type or mutant neurons (17, 41). Migration distances in neurons transfected with RFP-CRE alone were positioned indistinguishably from untransfected neurons, suggesting that RFP-CRE transfection had no effect on migration (Fig. 8A and D).[12] Overexpression of LIS1-GFP led to a mild increase in neuronal migration (Fig. 8A and D), as previously reported (41), whereas GFP-NDEL1 or GFP-NDE1 overexpression had no such effect (Fig. 8A,D). *Lis1*-null granule neurons displayed severe migration defects compared to wild-type neurons, characterized by a leftward shift of the bin distribution of migration distance, and the mean distance decreased by ~60% from the WT level (Fig. 8B and D). This migration defect due to *Lis1* inactivation was efficiently rescued by exogenous expression of GFP-LIS1 (Fig. 8B and D) but not by GFP-NDEL1 or GFP-NDE1.

Similar migration defects were observed in *Ndel1*-null neurons (Fig. 8C and D). This migration defect due to loss of *Ndel1* was rescued by exogenous expression of GFP-NDEL1 (Fig. 8C and D). GFP-LIS1 expression only moderately rescued the migration defect. More interestingly, GFP-NDE1 expression partially but incompletely rescued the migration defect derived from loss of *Ndel1*. The reduced magnitude of rescue suggests that NDEL1 and NDE1 have similar functions, but NDEL1 might have a more crucial and distinct function. These data are consistent with the early embryonic lethality displayed by *Ndel1*-null mice compared to the viable phenotype of *Nde1*-null mice, as well as the less-efficient recovery of disorganized microtubule network in *Ndel1*-null MEFs by GFP-NDE1 expression.

DISCUSSION

Ndel1 is one of the mouse homologues of Nude from *Aspergillus*, which was identified as a multicopy suppressors of a mutation in the *nudF* gene, the *Aspergillus* homologue of *LIS1* (6). NudE is also a homologue of the nuclear distribution protein RO11 (24) of *Neurospora crassa* and mitotic phosphoprotein 43 of *Xenopus laevis* (6). LIS1 and NDEL act in the CDHC pathway, which is the large molecular motor that translocates to the minus (−) ends of microtubules. Dynein, whose motor domain comprises six AAA modules and two potential mechanical levers, generates movement by a mechanism that is fundamentally different than that which underlies the motion of myosin and kinesin. CDHC is involved in numerous functions, including microtubule organization, vesicle transport (especially from the endoplasmic reticulum to the Golgi apparatus), chromosome separation, and nuclear distribution (12, 16, 45, 46).

To understand the in vivo role of NDEL1, we generated *Ndel1*-disrupted mice. Complete loss of NDEL1 caused embryonic lethality at the peri-implantation stage and a deficiency of cell proliferation in the inner cell mass. These data suggest that NDEL1-dependent regulation of CDHC is essential for proliferation and may play a role in important aspects of mitosis. Compared to *Lis1*$^{+/-}$ mice, which displayed clear neu-

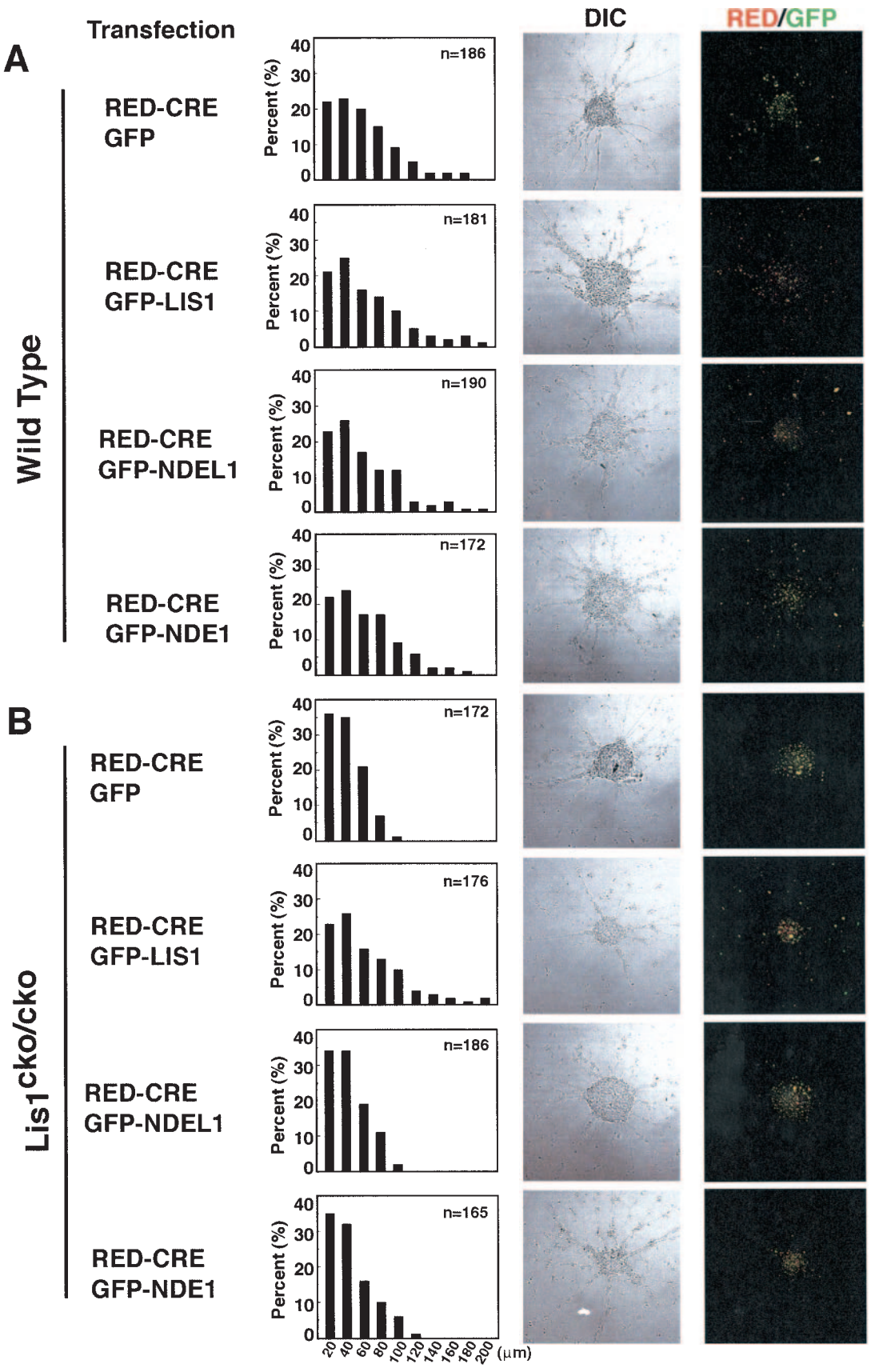
A
Transfection
Wild Type
RED-CRE
GFP
RED-CRE
GFP-LIS1
RED-CRE
GFP-NDEL1
RED-CRE
GFP-NDE1
B
Lis1cko/cko
RED-CRE
GFP
RED-CRE
GFP-LIS1
RED-CRE
GFP-NDEL1
RED-CRE
GFP-NDE1
DIC
RED/GFP
Percent (%)
n=186
n=181
n=190
n=172
n=172
n=176
n=186
n=165
0
10
20
30
40
20
40
60
80
100
120
140
160
180
200
(μm)

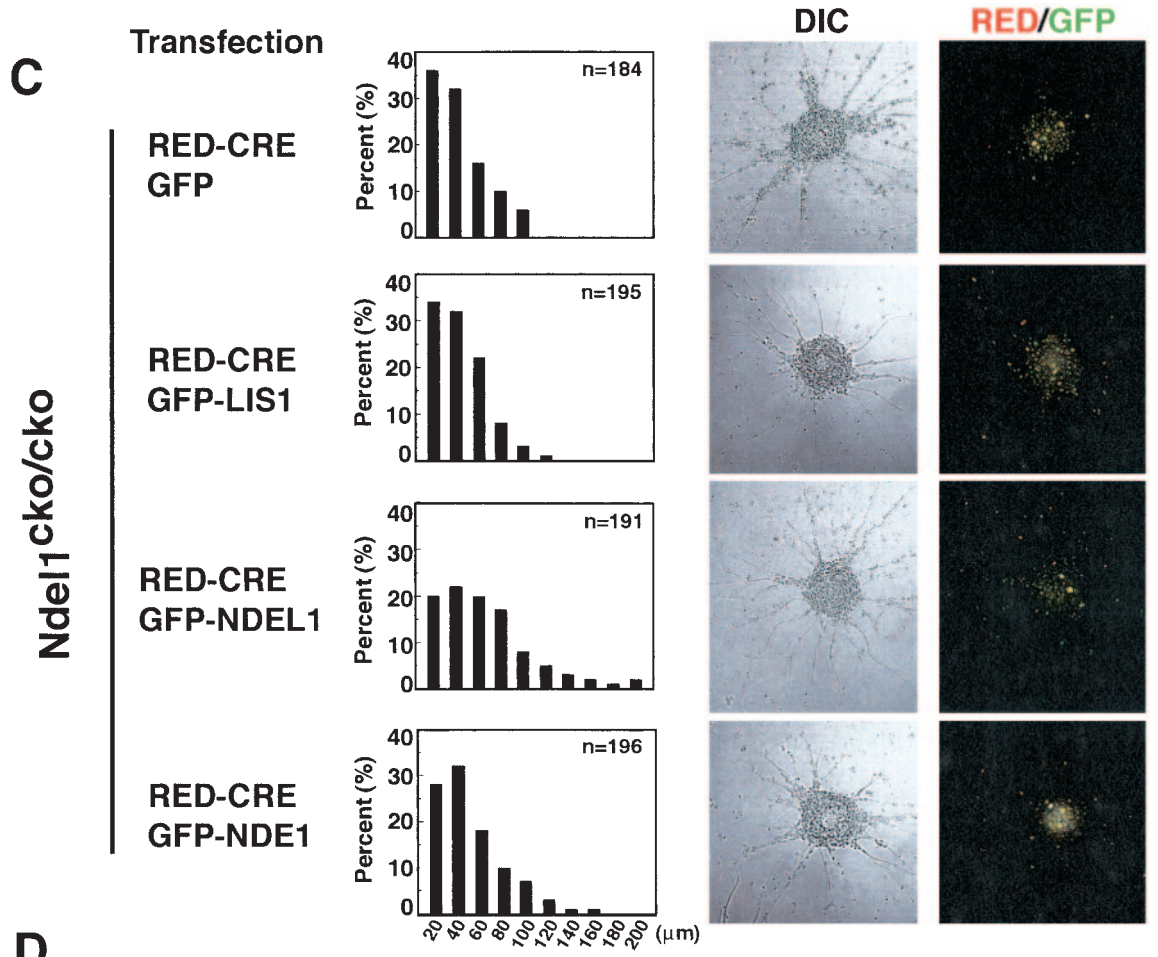
C
Transfection
Ndel1cko/cko
RED-CRE GFP
RED-CRE GFP-LIS1
RED-CRE GFP-NDEL1
RED-CRE GFP-NDE1
Percent (%)
n=184
n=195
n=191
n=196
(μm)
DIC
RED/GFP

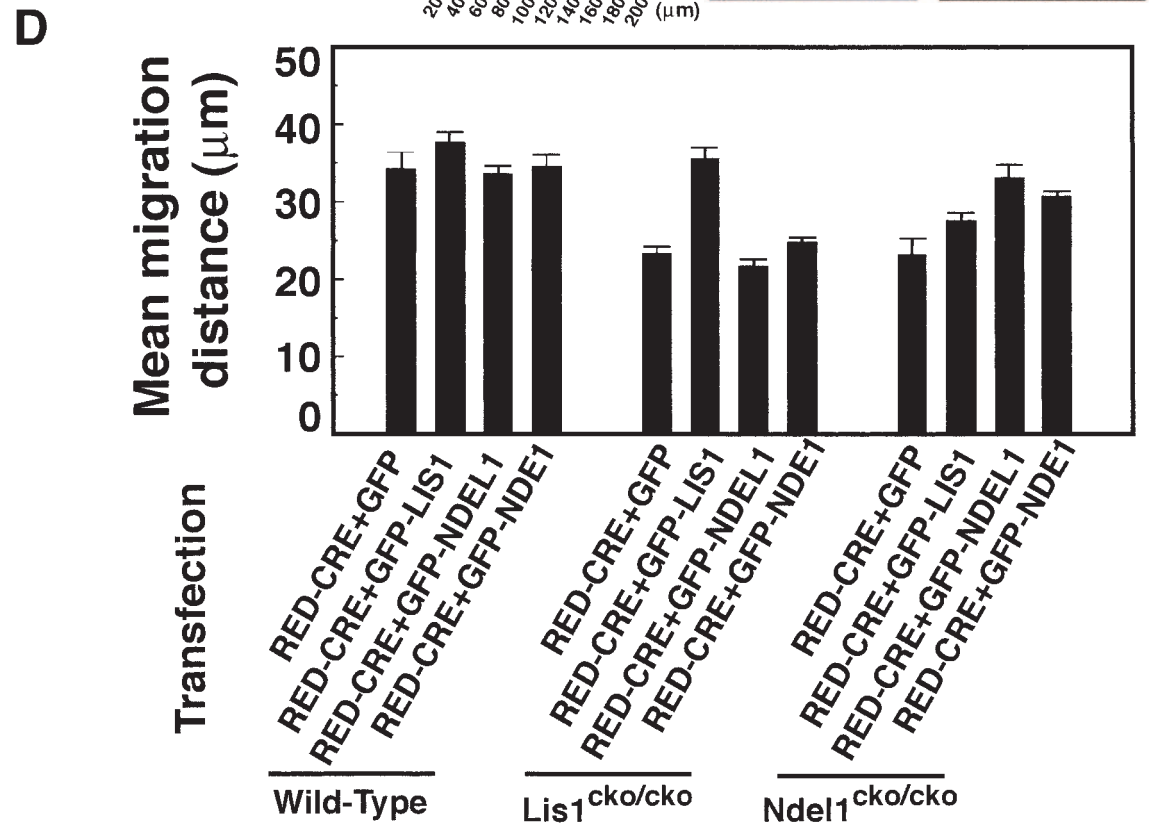
D
Mean migration distance (μm)
Transfection
RED-CRE+GFP
RED-CRE+GFP-LIS1
RED-CRE+GFP-NDEL1
RED-CRE+GFP-NDE1
Wild-Type
Lis1cko/cko
Ndel1cko/cko

ronal migration defects (10, 17), *Ndel1*$^{+/-}$ mice did not exhibit obvious phenotypes. Further reduction of *Ndel1* using a hypomorphic conditional allele resulted in mild neuronal migration defects. Double *Lis1*/*Ndel1* mutants displayed more severe migration defect than single mutants, suggesting that *Lis1* and *Ndel1* genetically interact. Elevated apoptotic cell death during neurogenesis was observed in *Lis1* mutants, whereas mutation of *Ndel1* did not result in apoptosis. We also examined LIS1 and NDEL1 functions on dynein regulation and microtubule organization. *Lis1*- and *Ndel1*-null MEFs displayed similar disruption of the compact juxtanuclear Golgi complex of β-COP-positive vesicles. The aberrant distribution of β-COP-positive vesicles in *Lis1*-null MEFs was only rescued by exogenous introduction of GFP-LIS1, while the disrupted organization of β-COP-positive vesicles in *Ndel1*-null MEFs was efficiently rescued by GFP-NDE1, as well as GFP-NDEL1, and it was partially rescued by GFP-LIS1. *Lis1* disruption resulted in pernuclear accumulation of microtubules, whereas *Ndel1* inactivation displayed amorphous distribution of microtubules. We also demonstrated that the disorganized microtubule network in *Ndel1*-null cells was completely rescued by GFP-NDEL1 but only partially rescued by GFP-LIS1 and GFP-NDE1. These results were similar to those found for neuronal migration using cerebellar granule cell reaggregation assays. Neuronal migration defects displayed by *Ndel1*-null neurons were completely rescued by GFP-NDEL1 but only partially rescued by GFP-LIS1 or GFP-NDE1 exogenous expression. Our data suggest that NDEL1, LIS1, and NDE1 act in a common pathway to regulate dynein but that each has distinct roles in the regulation of microtubule organization and neuronal migration.

Neuronal migration is the critical cellular process which initiates corticogenesis of cerebral cortex. Upon becoming postmitotic after their final mitosis, neurons migrate from the ventricular zone toward the cortical plate and then establish neuronal lamina via an "inside-out" gradient of maturation. Mutations of genes involved in neuronal migration result in defects of corticogenesis. *Lis1*$^{+/-}$ mutants display recognizable neuronal migration defects. In contrast, *Ndel1*$^{+/-}$ mutants exhibited no obvious phenotypes, *Ndel1*$^{cko/-}$ mutants exhibited clear aberration of neuronal migration, although the phenotype was milder than the phenotype of *Lis*$^{cko/-}$ mutants. We also demonstrated synergistic regulation of neuronal migration by LIS1 and NDEL1 using various crosses of *Lis1* and *Ndel1* mutants, suggesting that LIS1 and NDEL1 at least partially share the same pathway during neuronal migration. A recent report indicated that loss of function of *Ndel1*, *Lis1*, or dynein by RNA interference in the developing neocortex impairs neuronal positioning and causes the uncoupling of the centrosome and nucleus. These observations support our conclusion that LIS and NDEL1 share a common neuronal migration pathway (38).

In the developing central nervous system apoptosis plays an important role in the normal organization of the neuronal circuit. Roughly half of all of the neurons produced during neurogenesis die apoptotically before the nervous system matures (22). We have demonstrated that apoptotic cell death is significantly elevated in *Lis1* mutants. Apoptotic cell death was restricted to the ventricular zone, suggesting that LIS1 is essential for cell division of neuronal stem cells. Interestingly, neurons generated later were more sensitive to the reduction of LIS1. Long-lasting reduction of LIS1 might cause deregulation of proliferation and/or accumulation of disorganized organellar distribution that might trigger apoptosis or increase sensitivity to apoptotic inducers. Although migration defects were observed in brains from *Ndel1*$^{cko/-}$ mice, apoptotic cell death was not observed.

Another recent report demonstrated that the targeted disruption of the second homologue of NudE, *Nde1*, resulted in viable mice with a small brain (microcephaly) phenotype, with the most dramatic reduction affecting the cerebral cortex (9). In *Nde1* mutants (*Nde1*$^{-/-}$), cortical lamination was mostly preserved, but the mutant cortex had fewer neurons and very thin superficial cortical layers (II to IV). The small cerebral cortex is thought to reflect both reduced progenitor cell division and altered neuronal cell fates. In contrast to *Nde1*, complete loss of *Ndel1* resulted in perimplanation lethality, a phenotype similar to complete loss-of-function of *Lis1* (17) and *Cdhc* (14). *Ndel1* mutants more clearly displayed neuronal migration defect than *Nde1* mutants. These phenotypic differences between two homologues could be attributed to differences in the pattern and levels of expression during development (8, 29, 35, 36). NDE1 is expressed mainly in neuronal stem cells and is downregulated in the postmitotic neurons. In contrast, NDEL1 is first expressed in first in the early embryo. Later, NDEL1 is expressed in neuronal stem cells, and its expression continues in postmitotic neurons, suggesting that NDEL1 plays a broader role during development than NDE1. Another nonexclusive possibility is that NDEL1 has distinct molecular targets from NDE1. This possibility is supported by our observations that the disorganized microtubule network seen in the NDEL1-null MEFs was not completely rescued by NDE1 expression. Partial rescue of neuronal migration defect in NDEL1-null neurons by NDE1 introduction also supports this possibility. Further experiments with mutant mice for each of these components, which are now all available, as well as further biochemical studies, will provide more detailed explanations to address the similarities and differences in the roles

FIG. 8. Migration distance in *Lis1*- or *Ndel1*-null neurons determined by reaggregation assay. Granular neurons were isolated from P3 neonatal pups and subjected to the neuronal migration reaggregation assay. *Lis1* or *Ndel1* was inactivated by CRE-mediated recombination. Cotransfected plasmids for rescue are shown on the left side. The migration distance of each neurons after 12 h was binned. (A) Wild-type neurons expressing RFP-CRE display normal migration distance compared to untransfected neurons. Cotransfection of GFP-LIS1 mildly enhanced migration, whereas GFP-NDEL1 or GFP-NDE1 did not have obvious effect. (B and C) *Lis1* (B)- or *Ndel1* (C)-null neurons display a shift in the distribution of bins toward the right. Migration defects in *Lis1*-null neurons were only rescued by exogenous expression of GFP-LIS1. Migration defects in *Ndel1*-null neurons were rescued by exogenous expression of GFP-LIS1, GFP-NDEL1, and GFP-NDE1, but GFP-LIS1 and GFP-NDE1 were less effective (see panel C). Mean migration distances are summarized at the bottom. *n*, Number of neurons measured for each examination. (D) Summary of mean migration distance of each genotype.

of LIS1, NDEL1, and NDE1 in the regulation of dynein function and microtubule organization, as well as their roles in proliferation, neurogenesis, and neuronal migration.

ACKNOWLEDGMENTS

We thank Yoshihiko Funae, Hiroshi Iwao, Toshio Yamauch, Yoshitaka Nagai, and L. Robert Nussbaum for generous support and encouragement. We are grateful to Yuzuru Yamauchi, Shino Okumura, Michiyo Ishida, Katsumi Hagiwara, Nobuko Tominaga, Masami Suzuki, and Masashi Harada for mouse breeding and technical support. We thank Shin-ichi Hisanaga for providing a recombinant protein of cdk5/p35 and Francis J. MacNally for providing mutated kinesin.

This study was supported by NIH grant NS41030 to A.W.-B. and Grants-in-Aid for Scientific Research from the Ministry of Education, Science, Sports, and Culture of Japan to A.Y., K.T., and S.H. This study was also supported by Nissan Science Foundation grants to K.T. and a Sankyo Foundation of Life Science and Japan Brain Foundation grant to S.H.

REFERENCES

1. **Chae, T., Y. T. Kwon, R. Bronson, P. Dikkes, E. Li, and L. H. Tsai.** 1997. Mice lacking p35, a neuronal specific activator of Cdk5, display cortical lamination defects, seizures, and adult lethality. Neuron **18:**29–42.
2. **Deng, C., A. Wynshaw-Boris, F. Zhou, A. Kuo, and P. Leder.** 1996. Fibroblast growth factor receptor 3 is a negative regulator of bone growth. Cell **84:**911–921.
3. **Dobyns, W. B.** 1987. Developmental aspects of lissencephaly and the lissencephaly syndromes. Birth Defects **23:**225–241.
4. **Dobyns, W. B., O. Reiner, R. Carrozzo, and D. H. Ledbetter.** 1993. Lissencephaly: a human brain malformation associated with deletion of the *LIS1* gene located at chromosome 17p13. JAMA **23:**2838–2842.
5. **Donaldson, J. G., J. Lippincott-Schwartz, G. S. Bloom, T. E. Kreis, and R. D. Klausner.** 1990. Dissociation of a 110-kD peripheral membrane protein from the Golgi apparatus is an early event in brefeldin A action. J. Cell Biol. **111:**2295–2306.
6. **Efimov, V. P., and N. R. Morris.** 2000. The LIS1-related NUDF protein of *Aspergillus nidulans* interacts with the coiled-coil domain of the NUDE/RO11 protein. J. Cell Biol. **150:**681–688.
7. **Faulkner, N. E., D. L. Dujardin, C. Y. Tai, K. T. Vaughan, C. B. O'Connell, Y. Wang, and R. B. Vallee.** 2000. A role for the lissencephaly gene LIS1 in mitosis and cytoplasmic dynein function. Nat. Cell Biol. **2:**784–791.
8. **Feng, Y., E. C. Olson, P. T. Stukenberg, L. A. Flanagan, M. W. Kirschner, and C. A. Walsh.** 2000. Interactions between LIS1 and mNudE, a central component of the centrosome, are required for CNS lamination. Neuron **28:**665–679.
9. **Feng, Y., and C. A. Walsh.** 2004. Mitotic spindle regulation by *nde1* controls cerebral cortical size. Neuron **44:**279–293.
10. **Gambello, M. J., D. L. Darling, J. Yingling, T. Tanaka, J. G. Gleeson, and A. Wynshaw-Boris.** 2003. Multiple dose-dependent effects of Lis1 on cerebral cortical development. J. Neurosci. **23:**1719–1729.
11. **Gilmore, E. C., T. Ohshima, A. M. Goffinet, A. B. Kulkarni, and K. Herrup.** 1998. Cyclin-dependent kinase 5-deficient mice demonstrate novel developmental arrest in cerebral cortex. J. Neurosci. **18:**6370–6377.
12. **Gee, M. A., J. E. Heuser, and R. B. Vallee.** 1997. An extended microtubule-binding structure within the dynein motor domain. Nature **390:**636–639.
13. **Gupta, A., L. H. Tsai, and A. Wynshaw-Boris.** 2002. Life is a journey: a genetic look at neocortical development. Nat. Rev. Genet. **3:**342–355.
14. **Harada, A., Y. Takei, Y. Kanai, Y. Tanaka, S. Nonaka, and N. Hirokawa.** 1998. Golgi vesiculation and lysosome dispersion in cells lacking cytoplasmic dynein. J. Cell Biol. **141:**51–59.
15. **Hattori, M., H. Adachi, M. Tsujimoto, H. Arai, and K. Inoue.** 1994. Miller-Dieker lissencephaly gene encodes a subunit of brain platelet-activating factor acetylhydrolase. Nature **370:**216–218.
16. **Helfand, B. T., A. Mikami, R. B. Vallee, and R. D. Goldman.** 2002. A requirement for cytoplasmic dynein and dynactin in intermediate filament network assembly and organization. J. Cell Biol. **157:**795–806.
17. **Hirotsune, S., M. W. Fleck, M. J. Gambello, G. J. Bix, A. Chen, G. D., Clark, D. H. Ledbetter, C. J. McBain, and A. Wynshaw-Boris.** 1998. Graded reduction of Pafah1b1 (Lis1) activity results in neuronal migration defects and early embryonic lethality. Nat. Genet. **19:**333–339.
18. **Kwon, Y. T., and L. H. Tsai.** 2000. The role of the p35/cdk5 kinase in cortical development. Results Probl. Cell Differ. **30:**241–253.
19. **Lakso, M., J. G. Pichel, J. R. Gorman, B. Sauer, Y. Okamoto, E. Lee, F. W. Alt, and H. Westphal.** 1996. Efficient in vivo manipulation of mouse genomic sequences at the zygote stage. Proc. Natl. Acad. Sci. USA **93:**5860–5865.
20. **Liu, Z., T. Xie, and R. Steward.** 1999. Lis1, the *Drosophila* homologue of a human lissencephaly disease gene, is required for germline cell division and oocyte differentiation. Development **126:**4477–4488.
21. **Liu, Z., R. Steward, and L. Luo.** 2000. *Drosophila* Lis1 is required for neuroblast proliferation, dendritic elaboration and axonal transport. Nat. Cell Biol. **2:**776–783.
22. **Liu, D. X., and L. A. Greene.** 2001. Neuronal apoptosis at the G_1/S cell cycle checkpoint. Cell Tissue Res. **305:**217–228.
23. **Luskin, M. B., and C. J. Shatz.** 1985. Studies of the earliest generated cells of the cat's visual cortex: cogeneration of subplate and marginal zones. J. Neurosci. **99:**7881–7888.
24. **Miller, M. W., and F. A. Pitts.** 2000. Neurotrophin receptors in the somatosensory cortex of the mature rat: colocalization of p75, trk, isoforms and c-Neu. Brain Res. **852:**355–366.
25. **Minke, P. F., I. H. Lee, J. H. Tinsley, K. S. Bruno, and M. Plamann.** 1999. *Neurospora crassa* ro-10 and ro-11 genes encode novel proteins required for nuclear distribution. Mol. Microbiol. **32:**1065–1076.
26. **Morris, R. N., V. P. Efimov, and X. Xiang.** 1998. Nuclear migration, nucleokinesis, and lissencephaly. Trends Cell Biol. **8:**467–470.
27. **Morris, R. N.** 2000. Nuclear migration: from fungi to the mammalian brain. J. Cell Biol. **148:**1097–1101.
28. **Mullen, R. J., C. R. Buck, and A. M. Smith.** 1992. NeuN, a neuronal specific nuclear protein in vertebrates. Development **116:**201–211.
29. **Niethammer, M., D. S. Smith, R. Ayala, J. Peng, J. Ko, M. Lee, M. Morabito, and L. Tsai.** 2000. The Lis1 interacting protein Nude1 is a Cdk5 substrate that interacts with cytoplasmic dynein. Neuron **28:**697–711.
30. **Oshima, T., J. M. Ward, C. G. Huh, G. Longenecker, C. Veeranna, H. Pant, R. O. Brady, L. J. Martin, and A. B. Kulkarni.** 1996. Targeted disruption of the cyclin-dependent kinase 5 gene results in abnormal corticogenesis, neuronal pathology and perinatal death. Proc. Natl. Acad. Sci. USA **93:**11173–11178.
31. **Pliz, D. T., N. Matsumoto, S. Minnerath, P. Mills, and J. G. Glesson.** 1999. Lis1 and XLIS/doublecortin mutations cause most human classical lissencephaly, but different patterns if malformation. Hum. Mol. Genet. **7:**2029–2037.
32. **Rakic, P.** 1972. Model of cell migration to the superficial layers of fetal monkey neocortex. J. Comp. Neurol. **145:**61–83.
33. **Reiner, O., R. Carrozzo, Y. Shen, M. Wehnert, F. Faustinella, W. B. Dobyns, T. Caskey, and D. H. Ledbetter.** 1993. Isolation of a Miller-Dieker lissencephaly gene containing G protein b-subunit-like repeat. Nature **364:**717–721.
34. **Ringstedt, T., S. Linnarsson, J. Wagnoer, U. Lendahl, Z. Kokaia, E. Arenas, P. Ernfors, and C. F. Ibanez.** 1998. BDNF regulates reelin expression and Cajal-Retzius cell development in the cerebral cortex. Neuron **21:**305–315.
35. **Saito, T., R. Onuki, Y. Fujita, G. Kusakawa, K. Ishiguro, J. A. Bibb, T. Kishimoto, and S. Hisanaga.** 2003. Developmental regulation of the proteolysis of the p35 cyclin-dependent kinase 5 activator by phosphorylation. J. Neurosci. **23:**1189–1197.
36. **Sasaki, S., A. Shionoya, M. Ishida, M. J. Gambello, J. Yingling, A. Wynshaw-Boris, and S. Hirotsune.** 2000. A LIS1/NUDEL/cytoplasmic dynein heavy chain complex in the developing and adult nervous system. Neuron **28:**681–696.
37. **Sheppard, A. M., and A. L. Pearlman.** 1997. Abnormal organization of preplate neurons and their associated extracellular matrix: an early manifestation of altered neocortical development in the reeler mutant mouse. J. Comp. Neurol. **378:**173–179.
38. **Shu, T., R. Ayala, M. D. Nguyen, Z. Xie, J. G. Gleeson, and L. H. Tsai.** 2004. Ndel1 operates in a common pathway with LIS1 and cytoplasmic dynein to regulate cortical neuronal positioning. Neuron **44:**263–277.
39. **Smith, D. S., M. Niethammer, R. Ayala, Y. Zhou, M. J. Gambello, A. Wynshaw-Boris, and L.-H. Tsai.** 2000. Regulation of cytoplasmic dynein behaviour and microtubule organization by mammalian Lis1. Nat. Cell Biol. **2:**767–775.
40. **Swan, A., T. Nguyen, and B. Suter.** 1999. *Drosophila* lissencephaly-1 functions with Bic-D and dynein in oocyte determination and nuclear positioning. Nat. Cell Biol. **1:**444–449.
41. **Tanaka, T., Serneo, C. F. F. Higgins, M. J. Gambello, A. Wynshaw-Boris, and J. G. Gleeson.** 2004. Lis1 and doublecortin function with dynein to mediate coupling of the nucleus to the centrosome in neuronal migration. J. Cell Biol. **165:**709–721.
42. **Toyo-oka, K., A. Shionoya, M. J. Gambello, C. Cardoso, R. Leventer, H. L. Ward, R. Ayala, L. H. Tsai, W. Dobyns, D. Ledbetter, S. Hirotsune, and A. Wynshaw-Boris.** 2003. 14-3-3epsilon is important for neuronal migration by binding to NUDEL: a molecular explanation for Miller-Dieker syndrome. Nat. Genet. **34:**274–285.
43. **Trommsdorff, M., M. Gotthardt, T. Hiesberger, J. Shelton, W. Stockinger, J. Nimpf, R. E. Hammer, J. A. Richardson, and J. Herz.** 1999. Reeler/Disabled-like disruption of neuronal migration in knockout mice lacking the VLDL receptor and ApoE receptor 2. Cell **97:**689–701.
44. **Xiang, X., A. H. Osmani, S. A. Osmani, M. Xin, and N. R. Morris.** 1995. NudF, a nuclear migration gene in *Aspergillus nidulans*, is similar to the human LIS-1 gene required for neuronal migration. Mol. Biol. Cell **6:**297–310.
45. **Vallee, R. B., J. S. Wall, B. M. Paschal, and H. S. Shpetner.** 1988. Microtubule-associated protein 1C from brain is a two-headed cytosolic dynein. Nature **332:**561–563.
46. **Vallee, R. B., and M. P. Sheetz.** 1996. Targeting of motor proteins. Science **271:**1539–1544.
47. **Willins, D. A., B. Liu, X. Xiang, and N. R. Morris.** 1997. Mutations in the heavy chain of cytoplasmic dynein suppress the nudF nuclear migration mutation of *Aspergillus nidulans*. Mol. Gen. Genet. **255:**194–200.